

Supporting Information

A poly(ethylene glycol)-brush decorated magnetic polymer for highly specific enrichment of phosphopeptides

Liang Zhao, Hongqiang Qin, Zhengyan Hu, Yi Zhang, Ren'an Wu and Hanfa Zou**

National Chromatographic R&A Center, CAS Key Laboratory of Separation Sciences for Analytical Chemistry, Dalian Institute of Chemical Physics, Chinese Academy of Sciences (CAS), Dalian 116023, China

*To whom correspondence should be addressed:

Prof. Dr. Ren'an Wu

Tel: +86-411-84379576, Fax: +86-411-84379620, Email: wurenan@dicp.ac.cn

&

Prof. Dr. Hanfa Zou

Tel: +86-411-84379610, Fax: +86-411-84379620, E-mail: hanfazou@dicp.ac.cn

Table S1. Zeta-potential results of $\text{Fe}_3\text{O}_4@\text{SiO}_2@\text{PEG-Br}^{-1}$, amine functionalized $\text{Fe}_3\text{O}_4@\text{SiO}_2@\text{PEG}$ nanoparticles ($\text{Fe}_3\text{O}_4@\text{SiO}_2@\text{PEG-NH}_2$), phosphonate-modified $\text{Fe}_3\text{O}_4@\text{SiO}_2@\text{PEG}$ nanoparticles ($\text{Fe}_3\text{O}_4@\text{SiO}_2@\text{PEG-PO}_3^{2-}$), and $\text{Fe}_3\text{O}_4@\text{SiO}_2@\text{PEG-Ti}^{4+}$ nanoparticles for the subsequent modification reactions.

Functional nanoparticles	Zeta potential(mV)
$\text{Fe}_3\text{O}_4@\text{SiO}_2@\text{PEG-Br}^{-1}$	-3.73
$\text{Fe}_3\text{O}_4@\text{SiO}_2@\text{PEG-NH}_2$	+32.7
$\text{Fe}_3\text{O}_4@\text{SiO}_2@\text{PEG-PO}_3^{2-}$	-18.4
$\text{Fe}_3\text{O}_4@\text{SiO}_2@\text{PEG-Ti}^{4+}$	+17.2

Table S2. The surface compositions of functionalized PEG-decorated magnetic nanoparticle were determined by X-ray photoelectron spectroscopy (XPS) analysis. The C/O ratios for the poly(ethylene glycol) methacrylate brushes of $\text{Fe}_3\text{O}_4@\text{SiO}_2@\text{PEG}$ nanoparticles (great than the sampling depth of XPS) was 2.3, which is reasonably consistent with the stoichiometry value 2.1 of poly(ethylene glycol) methacrylate. The change of chemical compositions of functionalized PEG-decorated magnetic nanoparticles and the appearance of P and Ti element indicated the $\text{Fe}_3\text{O}_4@\text{SiO}_2@\text{PEG-Ti}^{4+}$ nanoparticles were successfully synthesized through multiply reactions.

Functional nanoparticles	XPS chemical compositions (%)						
	C	O	N	Si	Fe	P	Ti
$\text{Fe}_3\text{O}_4@\text{SiO}_2@\text{PEG}$	67.71	29.28	1.94	0.90	0.17		
$\text{Fe}_3\text{O}_4@\text{SiO}_2@\text{PEG-NH}_2$	71.27	25.40	2.16	1.04	0.13		
$\text{Fe}_3\text{O}_4@\text{SiO}_2@\text{PEG-PO}_3^{2-}$	61.12	32.26	2.68	0.81	0.11	2.02	
$\text{Fe}_3\text{O}_4@\text{SiO}_2@\text{PEG-Ti}^{4+}$	44.04	43.43	1.66	0.88	0.11	0.92	8.95

Table S3. Sequences of four standard phosphopeptides and identified phosphopeptides from α -casein, β -casein and ovalbumin tryptic digest MALDI-TOF MS analysis.

Protein	No.	Amino acid sequence	No. of phosphosite	[M+H] ⁺
α -Casein	α_1	TVDME[pS]TEVF	1	1237.08
	α_2	TVD[Mo]ME[pS]TEVF ^a	1	1253.11
	α_3	EQL[pS]T[pS]EENSK	2	1411.90
	α_4	VPQLEIVPN[pS]AEER	1	1660.15
	α_5	YLGEYLIVPN [pS]AEER	1	1832.70
	α_6	DIGSE[pS]TEDQAMEDIK	1	1847.95
	α_7	DIG[pS]E[pS]TEDQAMEDIK	2	1927.89
	α_8	DIG[pS]E[pS]TEDQA[Mo]EDIK ^a	2	1943.89
	α_9	YKVPQLEIVPN[pS]AEER	1	1951.09
	α_{10}	KKYKVPQLEIVPN[pS]AEERL	1	2080.00
	α_{11}	NTMEHV[pS][pS][pS]EESII[pS]QETYSK	4	2618.93
	α_{12}	VNEL[pS]KDIG[pS]E[pS]TEDQAMEDIK	3	2678.02
	α_{13}	Q*MEAE[pS]I[pS] [pS] [pS]EEIVPN[pS]VEAQK ^b	5	2703.75
	α_{14}	QMEAE[pS]I[pS][pS][pS]EEIVPNPN[pS]VEQK	5	2720.05
	α_{15}	Q[Mo]EAE[pS]I[pS][pS][pS]EEIVPNPN[pS]VEQK	5	2736.05
	α_{16}	KEKVNEL[pS]KDIG[pS]E[pS]TEDQAMEDIKQ	3	2935.87
	α_{17}	NANEEYSIG[pS][pS][pS]EE[pS]AEVATEEVK	4	3008.22
	α_{18}	NANEEY[pS]IG[pS][pS][pS]EE[pS]AEVATEEVK	5	3087.93
β -Casein	β_1	FQ[pS]EEQQQTEDELQDK	1	2061.94
	β_2	RELEELNVPGEIVE[pS]L[pS][pS][pS]EESITR	4	3122.56
Ovalbumin	O ₁	EVVG[pS]AEAGVDAASVSEEFR	1	2090.62
	O ₂	FDKLPFGFD[pS]IEAQCGTSVNVHSSLR	1	2903.46
---	S ₁	NVPL[pY]K	1	813.39
	S ₂	HLADL[pS]K	1	863.40
	S ₃	VNQIGTL[pS]E[pS]IK	2	1448.64
	S ₄	VNQIG[pT]LSESIK	1	1368.68

Notes: Superscripts: a) Oxidation on methionine; b) Pyroglutamylation on the N-terminal Q*.

Subscript: [pS] phosphorylated site.

Fig. S1 TGA curves of (a) $\text{Fe}_3\text{O}_4@\text{SiO}_2$; (b) $\text{Fe}_3\text{O}_4@\text{SiO}_2\text{-Br}$; (c) $\text{Fe}_3\text{O}_4@\text{SiO}_2@\text{PEG}$, respectively. TGA was carried out in nitrogen at a heating rate of $35^\circ\text{C}/10$ min. For the relative mass increase of $\text{Fe}_3\text{O}_4@\text{SiO}_2@\text{PEG}$ nanoparticles and $\text{Fe}_3\text{O}_4@\text{SiO}_2\text{-Br}$ nanoparticles were calculated from formula: $[(1 - W_{pp})/W_{pp} - (1 - W_{ip})/W_{ip}] \times 100\%$, where W_{pp} and W_{ip} represent the percent weight retention at 600°C of $\text{Fe}_3\text{O}_4@\text{SiO}_2@\text{PEG}$ nanoparticles and $\text{Fe}_3\text{O}_4@\text{SiO}_2\text{-Br}$ nanoparticles or $\text{Fe}_3\text{O}_4@\text{SiO}_2\text{-Br}$ nanoparticles and $\text{Fe}_3\text{O}_4@\text{SiO}_2$ nanoparticles, respectively. Assuming the magnetic nanoparticles were monodisperse with a spherical shape and considering the density of $\text{Fe}_3\text{O}_4@\text{SiO}_2$ was 5.18 g/cm^3 ¹, the grafting density of PEG brushes and initiator bromide were calculated according to a literature².

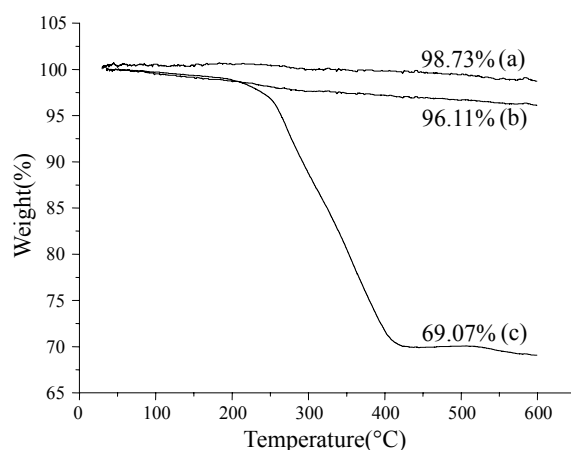


Fig. S2 FT-IR spectra of (a) $\text{Fe}_3\text{O}_4@\text{SiO}_2\text{-Br}$ (b) $\text{Fe}_3\text{O}_4@@\text{SiO}_2\text{PEG}$, respectively. Fig.S3a showed that the magnetite particles exhibit strong bands in the low-frequency region (440 and 578 cm^{-1}) due to the iron oxide skeleton, and the peaks of Si-O-Si stretching vibrations center at 1081 cm^{-1} ; the stretching vibrations of -C=O from amide occur at 1650 cm^{-1} , which confirms the attachment of initiator Br on the $\text{Fe}_3\text{O}_4@\text{SiO}_2$ nanoparticles. After large quantities of PEG brushes are grown on the surface of $\text{Fe}_3\text{O}_4@\text{SiO}_2\text{-Br}$ nanoparticles, the C-H stretching bands emerge at 2950 , 2870 cm^{-1} and the C=O stretching bands show a strong bands at 1720 cm^{-1} in the spectrum. The presence of C=O and CH_2 adsorption bands provide strong evidence that the PEG brushes were successfully coated on the $\text{Fe}_3\text{O}_4@\text{SiO}_2\text{-Br}$ nanoparticles.

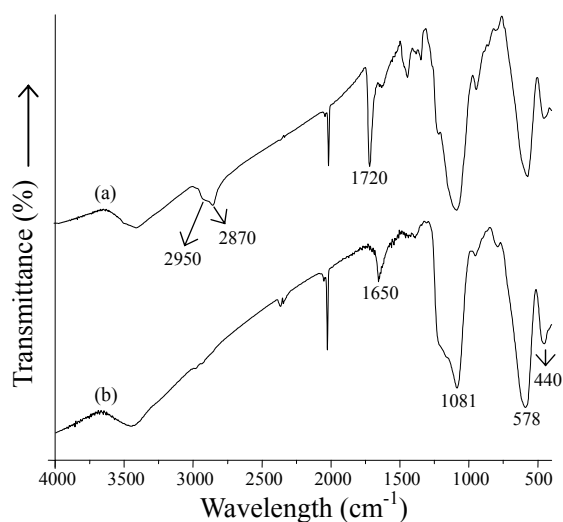


Figure S3. Wide-scan XPS spectra of the functionalized magnetic nanoparticles: (a) $\text{Fe}_3\text{O}_4@\text{SiO}_2@\text{PEG}$; (b) $\text{Fe}_3\text{O}_4@\text{SiO}_2@\text{PEG-NH}_2$; (c) $\text{Fe}_3\text{O}_4@\text{SiO}_2@\text{PEG-PO}_3^{2-}$; (d) $\text{Fe}_3\text{O}_4@\text{SiO}_2@\text{PEG-Ti}^{4+}$ magnetic nanoparticles.

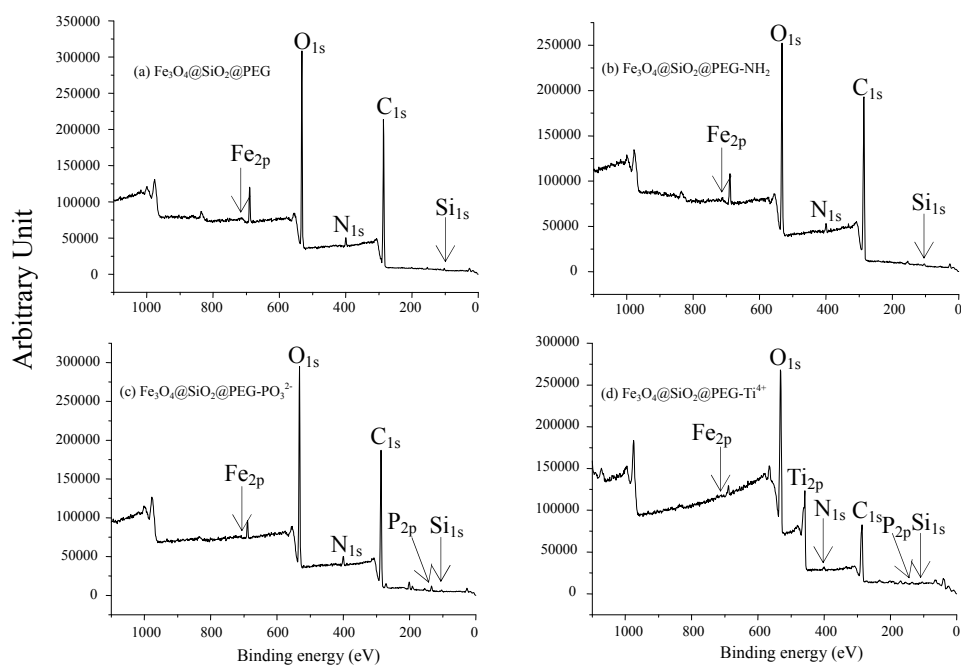


Fig. S4. The EDX spectrum data of $\text{Fe}_3\text{O}_4@\text{SiO}_2@\text{PEG-Ti}^{4+}$ magnetic nanoparticles.

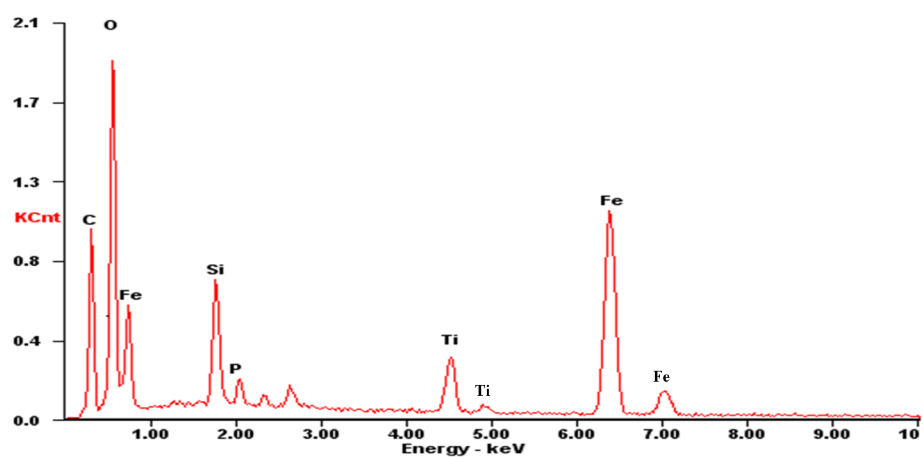


Fig. S5 The hysteresis loops of $\text{Fe}_3\text{O}_4@\text{SiO}_2@\text{PEG-Ti}^{4+}$ magnetic nanoparticles.

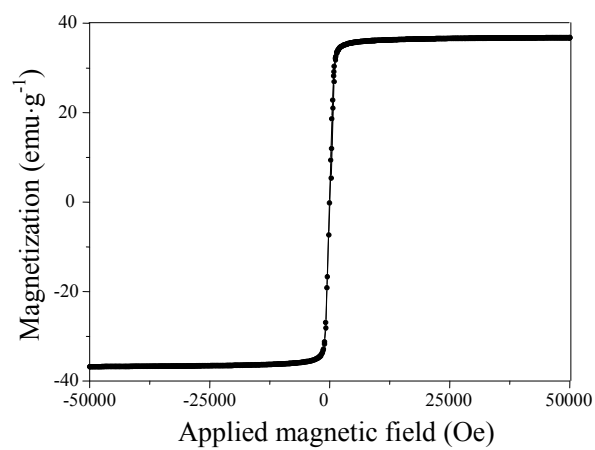


Fig. S6 MALDI-TOF MS analysis of tryptic digests of β -casein (200 μ L) enriched by $\text{Fe}_3\text{O}_4@\text{SiO}_2@\text{PEG-Ti}^{4+}$ (a,b,c) and $\text{Fe}_3\text{O}_4@\text{SiO}_2\text{-Ti}^{4+}$ (d,e,f) IMAC nanoparticles at different concentrations of (i) 1×10^{-10} M, (ii) 5×10^{-11} M and (iii) 2.5×10^{-11} M, respectively.

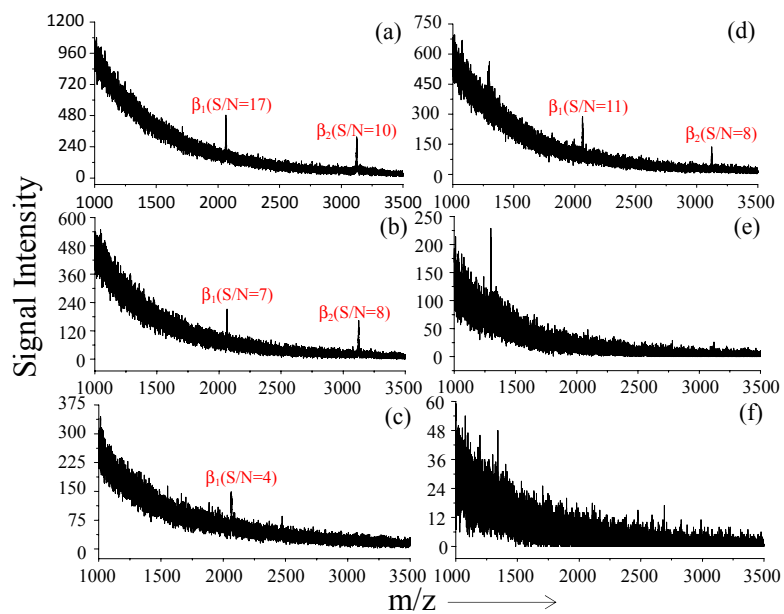
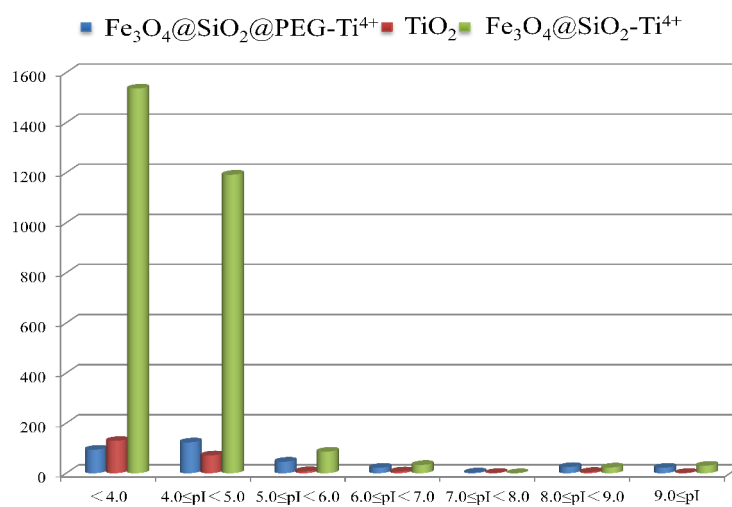


Fig. S7 The distribution of isoelectric points of nonphosphopeptides obtained by using $\text{Fe}_3\text{O}_4@\text{SiO}_2@\text{PEG-Ti}^{4+}$, $\text{Fe}_3\text{O}_4@\text{SiO}_2\text{-Ti}^{4+}$ IMAC nanoparticles and TiO_2 microspheres.



Literature :

1. R. Matsuno, K. Yamamoto, H. Otsuka and A. Takahara, *Macromolecules*, 2004, **37**, 2203-2209.
2. A. P. Majewski, A. Schallon, V. Jerome, R. Freitag, A. H. Muller and H. Schmalz, *Biomacromolecules*, 2012, **13**, 857-866.